

Proceedings from the Ninth International Zeolite Conference

Montreal
1992



Volume II

Edited by
R. von Ballmoos, J.B. Higgins and M.M.J. Treacy

VE 9600 BAL2 -2

Butterworth-Heinemann

Boston London Oxford Singapore Sydney Toronto Wellington

CONTENTS

VOLUME I

Preface:

Editors	<i>iii</i>
Chairman Executive Committee of the 9th IZC	<i>iv</i>
Executive Committee of the 9th IZC	<i>v</i>
Program Committee of the 9th IZC	<i>vi</i>
International Advisory Board to the 9th IZC	<i>vii</i>
Financial Support	<i>viii</i>

Keynote Lecture

Observations and Descriptions: On an Unknown Mineral-Species Called Zeolites, by Axel Fredrick Cronstedt John L. Schlenker and Günter H. Köhl	3
---	---

Plenary Lectures

Host/Guest Chemistry and Catalysis in Zeolites Jens Weitkamp	13
Ceramic Membranes for Separations and Reactions A.J. Burggraaf, K. Keizer, R.S.A. de Lange, Z.A.E.P. Vroon and V.T. Zaspalis	47
Recent Advances and Perspectives in Molecular Sieve Synthesis H. Kessler	73
Sodalite Supralattices: From Molecules to Clusters to Expanded Insulators, Semiconductors and Metals Andreas Stein and Geoffrey A. Ozin	93
Zeolite Structural Problems From a Computational Perspective J.M. Newsam	127
DISCUSSION – Plenary Lectures	143

Synthesis

The Role of Alkali Cations in the Syntheses of Silicalite-1 in Fluoride Medium F. Crea, R. Mostowicz, F. Testa, R. Aiello, A. Nastro and J.B. Nagy	147
Synthesis of NH₄-Form Heteroatom-Substituted MFI Zeolites in the Presence of Fluoride Anions John Dwyer, Jingping Zhao and David Rawlence	155
An Unexpected and Highly Versatile New Zeolite Synthesis Route Leading to Large Pore Alumino and Borosilicate Sieves S.I. Zones, L.T. Yuen, Y. Nakagawa, R.A. Van Nordstrand and S.D. Toto	163
Organic Guest Stabilization During Synthesis of High Silica Zeolites With Multidimensional Channels and Large Pores: SSZ-26 From a Propellane-Based Organocation S.I. Zones and D.S. Santilli	171
Raman Spectroscopic Studies in Zeolite Synthesis P.K. Dutta	181
Synthesis and Characterization of a New High-Silica, Large-Pore Aluminosilicate Zeolite, NCL-1 R. Kumar, K. Ramesh Reddy, Anuj Raj and P. Ratnasamy	189
Zeolite Synthesis in Ammonia and Aqueous Ammonia Solvents: Reactivity of Group IA Cations with Pre-Made Silica-Alumina Gels D.E.W. Vaughan and K.G. Strohmaier	197
Study on the Insertion of Vanadium in the Silicalite Framework G. Bellussi, G. Maddinelli, A. Carati, A. Gervasini and R. Millini	207
F⁻: A Multifunctional Tool for Microporous Solids a) Mineralizing, Structure Directing and Templating Effects in the Synthesis J.L. Guth, H. Kessler, P. Caullet, J. Hazm, A. Merrouche and J. Patarin	215
The Synthesis and Characterization of Ga-MFI and Ga-MTW Zeolites S.L. Lambert	223
Synthesis of Gallo- and Gallo-Alumino ZSM-5 Zeolites with Variable and Quasi-Homogeneous Al-Ga Distribution, From Alkali-Free Media Z. Gabelica, G. Giannetto, F. Dos Santos, R. Monque and R. Galiasso	231
Preparation of Zeolite Film Using Cellulose Moulding T. Sano, Y. Kiyozumi, K. Maeda, M. Toba, S. Niwa and F. Mizukami	239

Controlled Growth of Thin Films of Molecular Sieves on Various Supports J.C. Jansen, W. Nugroho and H. van Bekkum	247
Molecular Design of Layered Zirconium Phosphonate Catalysts K. Segawa, N. Kihara, H. Yamamoto and S. Nakata	255
Synthesis and Characterization of the Novel Gallophosphate Cloverite with 20-Membered Ring Channels J. Patarin, C. Schott, A. Merrouche, H. Kessler, M. Soulard, L. Delmotte, J.L. Guth and J.F. Joly	263
The Crystallization of Aluminophosphate Microporous Compounds in Alcoholic System Ruren Xu, Qisheng Huo and Wenqin Pang	271
Synthesis, Characterization and Phase Transition of the 20-Membered Ring $AlPO_4$: JDF-20 Qisheng Huo, Ruren Xu, Shougui Li, Yihua Xu, Zhanguo Ma, Yong Yue, Liyun Li	279
Hydrothermal Transformation of Zeolite ZSM-39 into ZSM-23 S. Ernst, R. Kumar and J. Weitkamp	287
Synthesis of Ultrafine Zeolite L Xianping Meng, Yan Zhang, Changgong Meng and Wenqin Pang	297
New Silica-Alumina with Nano-Scale Pores Prepared from Kanemite S. Inagaki, Y. Fukushima, A. Okada, T. Kurauchi, K. Kuroda and C. Kato	305
A Microporous Tetraethylammonium Permutite as Synthesis Intermediate of the Zeolite Beta M.A. Nicolle, F. di Renzo, F. Fajula, P. Espiau and T. des Courieres	313
Modeling and Simulation of Zeolite Crystallization B. Subotic and J. Bronic	321
Probing the Synthesis of $CoAPO-n$ Molecular Sieves by Analysis of Wet Precursor Gels M.G. Uytterhoeven and R.A. Schoonheydt	329
Zeolites Synthesized from Nonalkaline Media Daqing Zhao, Shilun Qiu and Wenqin Pang	337
A New Family of Microporous Germanium Dioxide Crystals Shougui Li, Ruren Xu, Yuqin Lu and Yihua Xu	345

Synthesis, Dealumination and Physico-Chemical Characterization of Zeolite EMT J. Weitkamp and R. Schumacher	353
---	-----

DISCUSSION – Synthesis	361
---	-----

Structure

Cation Distribution as a Structural-Chemical Probe J.L. Lievens and W.J. Mortier	373
--	-----

A Combinatorial Method for Generating New Zeolite Frameworks M.M.J. Treacy, S. Rao and I. Rivin	381
---	-----

Method of Solution and Structure of 3 Novel High-Silica Medium-Pore Zeolites with Multi-Dimensional Channel Systems M.D. Shannon	389
--	-----

Group 2(Be)/12(Zn)-15(P,As)O₄ Molecular Sieves William T.A. Harrison, Thurman E. Gier, Tina M. Nenoff and Galen D. Stucky	399
--	-----

Hydrogen Bonds Distort the Aluminosilicate Framework of Ammonium-Natrolite E. Stuckenschmidt, D. Kassner, W. Joswig and W.H. Baur	407
---	-----

Synthesis and Characterization of Breck Structure Six, Faujasite, ZSM-3, and ZSM-20 and their Structural Relationships G.W. Skeels, C.S. Blackwell, K.B. Reuter, N.K. McGuire and C.A. Bateman	415
--	-----

Single Crystal Structure Analysis of Zeolite Beta: The Superposition Structure B. Marler, R. Böhme and H. Gies	425
--	-----

Rietveld Refinement of F-Containing GaPO₄-LTA A. Simmen, J. Patarin and Ch. Baerlocher	433
---	-----

DISCUSSION – Structure	441
---	-----

Characterization

Titanium Silicalite-1 Peroxides M.G. Clerici, P. Ingallina and R. Millini	445
---	-----

Local Environment of Titanium in Titanium Silicalite (TS-2) A. Bittar, D. Trong On, L. Bonneviot, S. Kaliaguine and A. Sayari	453
Properties of Indium Containing Zeolites Prepared by a Solid State Reaction V. Kanazirev, Y. Neinska, T. Tsoncheva and L. Kosova	461
Spectroscopy, Energetics and Siting of NH₄⁺ in Zeolites: Theory and Experiment E.H. Teunissen, W.P.J.H. Jacobs, A.P.J. Jansen and R.A. van Santen	469
Studies on Template Molecules: Location, Orientation, Protonation and Interaction with Framework in High Silica Zeolites Yaojun Sun, Tailiu Wu, Liping Wang, Lun Fei and Yingcai Long	479
Electron Spin Echo Studies of Mn(II) Framework Substitution in MnAPO-11 Guillaume Brouet, Xinhua Chen and Larry Kevan	489
Elucidating the Morphology of Clays: HREM and ESEM Studies K.B. Reuter, J.J. Alcaraz, J.A. Triphahn, J.S. Holmgren	497
Characterisation and Catalytic Properties of Titanium Incorporated into Zeolites and Silicas From Titanium Trifluoride P.J. Kooyman, J.C. Jansen and H. van Bekkum	505
The Preparation, Characterisation and Properties of Zeolite NU-86 J.L. Casci, P.A. Cox and M.D. Shannon	513
Application of Diffuse Reflectance FTIR Spectroscopy in Molecular Sieve Research E. Loeffler, Ch. Peuker, B. Zibrowius, U. Zscherpel, K.-H. Schnabel	521
An Infrared Study of Structure Relaxation in Molecular Sieves W.P.J.H. Jacobs, A.J.M. de Man, J.H.M.C. van Wolput and R.A. van Santen	529
Quantum Chemical Interpretation of IR Data of Methanol Adsorption on Zeolites and Silica A.G. Pelmenschikov, G. Morosi and A. Gamba	537
The Influence of Quadrupolar Effect on High-Resolution ²⁷Al Double Rotation (DOR) NMR of Aluminophosphate Molecular Sieves P.J. Grobet, H. Geerts, J.A. Martens and P.A. Jacobs	545
NMR Studies of the Water Motion in AlPO₄-5, CoAlPO₄-5 and VPI-5 D. Goldfarb, I. Kustanovich and J.O. Perez	553

Solid State MAS NMR Characterization of the Transformation of VPI-5 to AlPO₄-8: Preservation of the Octahedral Aluminum Sites? D.E. Akporiaye and M. Stöcker	563
¹²⁹Xe NMR as a Probe of Structure and Dynamics In Microporous Solids J.A. Ripmeester and C.I. Ratcliffe	571
Zeolite Intrinsic Framework Reactivity and Sensitivity Analysis of Framework Perturbations B.G. Baekelandt, J.L. Lievens, W.J. Mortier and R.A. Schoonheydt	579
Dependence of Charge Density and Electric Field Within the Cages of X and Y Zeolites on the Cation: Photophysical Probes V. Ramamurthy and D.F. Eaton	587
Location of Iron in Framework-Substituted Zeolite L Using Anomalous Powder X-Ray Diffraction and X-Ray Absorption Fine Structure I.J. Pickering, D.E.W. Vaughan, K.G. Strohmaier, G.N. George and G.H. Via	595
Electron-Accepting Strength of Aluminum Species in H-Zeolites F.R. Chen and J.J. Fripiat	603
F⁻: A Multifunctional Tool for Microporous Solids b) ¹⁹F NMR of As-Synthesized and Post-Synthesis Treated Materials E. Klock, L. Delmotte, M. Soulard and J.L. Guth	611
Synchrotron Based Diffraction Studies of Sorption in Zeolite Y at Room Temperature Z.A. Kaszukur, J.W. Couves, R.H. Jones, D. Waller, C.R.A. Catlow and J.M. Thomas	619
Combined <i>In-Situ</i> X-Ray Powder Diffraction and X-Ray Absorption Spectroscopic Studies of Transition-Metal-Incorporated ALPO and SAPO Catalysts J.W. Couves, G. Sankar, J.M. Thomas, J. Chen, C.R.A. Catlow, R. Xu and G.N. Greaves	627
Correlations Between Acid Strength and Si Environment in Faujasite Type Molecular Sieves M. Briend and D. Barthomeuf	635
Template-Free and Alkali-Free Synthesized Silicates With MFI-Structure – A Comparative Study M. Wallau, F. Schüth, A. Brenner, S. Melson, R. Spichtinger, K. Unger, A. Tissler and B. Zibrowius	643

Spectroscopic Investigation of the Redox Properties of CoAPO Molecular Sieves
 M.P.J. Peeters, J.H.C. van Hooff, R.A. Sheldon, V.L. Zholobenko, L.M. Kustov and V.B. Kazansky 651

Effect of Dehydration and Cationic Exchange on the ²³Na and ⁷Li MAS NMR Spectra of X and Y Zeolites
 J.M. Chezeau, A. Saada, L. Delmotte and J.L. Guth 659

DISCUSSION – Structure 667

Modelling

Proton Transfer from Acidic Sites to Water, Methanol and Ammonia. A Comparative ab initio Study
 Joachim Sauer, Christoph Kolmel, Frank Haase and Reinhardt Ahlrichs 679

Siting of Al and Bridging Hydroxyl Groups in Zeolite Catalysts. Computer Simulations of Their Structure, Vibrational Spectra and Acidity
 K.-P. Schröder and J. Sauer 687

Structural and Dynamical Properties of Hydrocarbons in Silicalite
 E. Hernandez, M. Kawano, A.A. Shubin, C.M. Freeman, C.R.A. Catlow, J.M. Thomas and K.I. Zamaraev 695

Computer Modelling of Microporous Solids
 R.G. Bell, R.A. Jackson and C.R.A. Catlow 703

DISCUSSION – Modelling 709

Author Index (Volumes I and II) 711

Subject Index (Volumes I and II) 717

VOLUME II

Adsorption

Liquid-Phase-Adsorption of Binary Monosaccharide-Water and Polyol-Water Mixtures on X and Y Zeolites
 R. Schöllner, S. Unverricht and W.-D. Einicke 3

Zeolites as Media for Hydrogen Storage J. Weitkamp, M. Fritz and S. Ernst	11
Adsorption of Polar Molecules on the Large Pore Molecular Sieve VPI-5 J. Jänchen, H. Stach, P.J. Grobet, J.A. Martens and P.A. Jacobs	21
Adsorbent Filled Membranes for Gas Separation J.-M. Duval, B. Folkers, M.H.V. Mulder, G. Desgrandchamps and C.A. Smolders	29
Transport in Zeolites: Application of NMR to Probe Sorption Phenomena R.L. Portsmouth, M.J. Duer and L.F. Gladden	37
Diffusion of Benzene, <i>p</i>-Xylene and their Mixture in Silicalite-1 Using a Frequency Response Technique Dongmin Shen and Lovat V.C. Rees	45
Adsorption, Coadsorption and Diffusion of Isotopic Hydrogen Molecules in NaA Zeolite. Evidence for Quantum Effects at 80 K E. Cohen de Lara, R. Kahn, J.P. Bouchaud and H. Ibnass	55
A Study of the Dynamics of Aromatic Adsorbates in Faujasite-Type Zeolites L.M. Bull, S.J. Heyes and A.K. Cheetham	63
Molecular Simulations of Low Occupancy Adsorption of Aromatics in Silicalite R.Q. Snurr, A.T. Bell and D.N. Theodorou	71
The Hydrophobicity Index - A Valuable Test for Probing the Surface Properties of Zeolitic Adsorbents or Catalysts J. Weitkamp, P. Kleinschmit, A. Kiss and C.H. Berke	79
Separation of Gaseous Tetrachloroethene/Water Mixtures by Adsorption on Zeolites R. Schumacher, S. Ernst and J. Weitkamp	89
Application of the ZLC Method to the Measurement of Intracrystalline Counter-Diffusion in Liquid-Zeolite Systems D.M. Ruthven, P. Stapleton and K. Dahlke	97
A Monte-Carlo Simulation of Zeolitic Adsorbents During a Kinetically Controlled Pressure Swing Adsorption Process R.L. Portsmouth and L.F. Gladden	105
Sorption and Diffusion of Benzene in BaX-Type Zeolite M. Bülow, W. Mietk and M. Nywt	113

Translational Mobility of <i>n</i>-Butane and <i>n</i>-Hexane in ZSM-5 Measured by Quasi-Elastic Neutron Scattering H. Jobic, M. Bee and J. Caro	121
Diffusion Anisotropy and Single-File Diffusion in Zeolites J. Kärger and H. Pfeifer	129
Molecular Dynamics Simulations of Diffusion in Zeolites P. Demontis and G.B. Suffritti	137
Diffusion of Monatomic, Diatomic and Simple Polyatomic Sorbates in 5A and 13X Zeolite Crystals As Studied by the ZLC Method Zhige Xu, Mladen Eic and Douglas Ruthven	147
DISCUSSION – Adsorption	157

Solid State

Intrazeolite Chemistry of Organometallics with Methyl Ligands: Cyclopentadienyl Methyl Iridodicarbonyl Aticha Borvornwattananont and Thomas Bein	169
Synthesis of Oligo- and Polythiophenes in Zeolite Hosts Patricia Enzel and Thomas Bein	177
Stepwise Synthesis of II-VI Nanoclusters Inside Zeolite Y Supercages Using MOCVD Type Precursors Mark R. Steele, Andrew J. Holmes and Geoffrey A. Ozin	185
Zeolite Encapsulated Gadolinium(III) Chelate Complexes K.J. Balkus, Jr., I. Bresinska and S.W. Young	193
DISCUSSION – Solid State	203

Natural Zeolites

Reconstruction of a Natural Zeolitization Process Through Laboratory Simulations M. de' Gennaro, C. Colella, M. Pansini and A. Langella	207
Natural Zeolites in Environment Preservation: An Innovative Strategy for Chromium Removal M. Pansini, C. Colella, M. de' Gennaro and A. Langella	215

Characterization of the Clinoptilolite-Rich Tufts of Bigadiç: Variation of the Ion-Exchange Capacity with Pretreatments and Zeolite Content A. Erdem Senatalar, A. Sirkecioglu, I. Guray, F. Esenli and I. Kumbasar	223
---	-----

DISCUSSION – Natural Zeolites	231
--	-----

Acid Site Characterization

Acidic Properties of Al,Si-MFI Zeolites: Influence of the Synthesis Conditions (F^- or OH^-). An Infrared and Microcalorimetry Study J.F. Joly, A. Auroux, J.C. Lavalley, A. Janin and J.L. Guth	235
--	-----

The Formation of Stoichiometric Adsorption Complexes for Simple Thiols in H-ZSM-5 and H-ZSM-12 C. Pereira, R.J. Gorte and G.T. Kokotailo	243
--	-----

The Role of the Hardness of the Zeolite Lattice for the Local Adsorption Structure of Polar Molecules G. Mirth, A. Kogelbauer and J.A. Lercher	251
--	-----

The Quantitative Study of Brønsted Acidity in SAPO-37 M.A. Makarova, A.F. Ojo, K.M. Al-Ghefaily and J. Dwyer	259
--	-----

Assessment of Broensted Acidity in Zeolites by CO Adsorption: An IR Study E. Garrone, R. Chiappetta, G. Spoto, P. Ugliengo, A. Zecchina and F. Fajula	267
---	-----

IR Investigation of CO Physisorption at Low Temperature as a Probe for Bronsted Acidity in Zeolites N. Echoufi and P. Gelin	275
---	-----

ESR Measurements for the Characterization of Acidic Lewis Sites in Zeolites F. Witzel, H.G. Karge and A. Gutsze	283
---	-----

DISCUSSION – Acid Site Characterization	293
--	-----

Catalysis

The Role of Lewis Acid Sites in Adsorption and Activation of Oxygen in Redox Type Reactions on Zeolites V.L. Zholobenko, L.M. Kustov and V.B. Kazansky	299
--	-----

Zeolite Catalyzed Rearrangements of Epoxides and Glycidic Esters W.F. Hoelderich and N. Goetz	309
---	-----

In Situ FT-IR Study of Acid Sites Responsible for Cyclohexene Conversion on HY Zeolites S. Jolly, J. Saussey, J.C. Lavalley, N. Zanier, E. Benazzi and J.F. Joly	319
Cumene Production Based on Modified Mordenite Catalysts G.R. Meima, M.J.M. van der Aalst, M.S.U. Samson, J.M. Garces and J.G. Lee	327
Transformation of Propane over Ga/HZSM-5 Catalysts: On the Activation Procedure and the Nature of the Active Site P. Mériaudeau, G. Sappaly, M. Dufaux and C. Naccache	335
Modelization of SAPO-37 and Its Verification Through Physicochemical Characterization and Chemical Reactivity A. Corma, V. Fornes, M.J. Franco, F. Melo, J. Perez-Pariente and E. Sastre	343
Characterization of Large and Extra-Large Zeolite Pores with the Heptadecane Test J.A. Martens, G.M. Vanbutsele and P.A. Jacobs	355
Performance of Zeolite Beta in Friedel-Crafts Reactions of Functionalized Aromatics G. Harvey, A. Vogt, H.W. Kouwenhoven and R. Prins	363
Permeation Measurements on In Situ Grown Ceramic MFI Type Films E.R. Geus, W.J.W. Bakker, P.J.T. Verheijen, M.J. den Exter, J.A. Moulijn and H. van Bekkum	371
Soft and Hard Acidity in Zeolites and Zeotypes: Evaluation and Catalytic Implications A. Corma, E. Sastre, G. Sastre, P. Viruela and C. Zicovich	379
Isomerization of Light Paraffins on Mordenite, Mazzite and Beta. Relationship Between Acidity and Catalytic Activity M. Boulet, E. Bourgeat-Lami, F. Fajula, T. Des Courieres and E. Garrone	389
Selective Reduction of NO by Hydrocarbon in O₂ on Metal Ion-Exchanged Zeolite Catalysts Masakazu Iwamoto, Hidenori Yahiro and Noritaka Mizuno	397
Decomposition of NO on Metallosilicates Under an Excess of Oxygen and a Low Concentration of Hydrocarbons T. Inui, S. Iwamoto and S. Shimizu	405
Influence of Hydrogen Sulfide and of Ammonia on the Hydrocracking of <i>n</i>-Heptane over a NiMo/Y Zeolite Catalyst M. Guisnet, J.L. Lemberon, C. Thomazeau and S. Mignard	413

Inhibited Deactivation of Pt Sites and Selective Dehydrocyclization of <i>n</i>-Heptane within L-Zeolite Channels Enrique Iglesia and Joseph E. Baumgartner	421
The Influence of Hydrogen Pretreatment on the Structural and Catalytic Properties of a Pt/K-LTL Catalyst M. Vaarkamp, J. van Grondelle, R.A. van Santen, J.T. Miller, B.L. Meyers, F.S. Modica, G.S. Lane and D.C. Koningsberger	433
Characterization of Pt-Ni/KL-Zeolite Bimetallic Catalysts by Chemisorption, Catalysis and X-Ray Absorption Gustavo Larsen and Gary L. Haller	441
Alkylation of Benzene with Propylene over SAPO-5, SAPO-11 and SAPO-37 I.I. Ivanova, N. Dumont, Z. Gabelica, J.B. Nagy, E.G. Derouane, F. Ghigny, O.E. Ivashkina, E.V. Dmitruk, A. Smirnov and B.V. Romanovsky	449
The Influence of Diffusion Limitations on Xylene Isomerization J.A. Amelse	457
The Effect of Oxygenates on the Propene Oligomerization Activity of ZSM-5 C.T. O'Connor, S.T. Langford and J.C.Q. Fletcher	467
Study by ¹²⁹Xe and ²⁷Al N.M.R. Spectroscopy of the Interactions of Coke with Aluminum Species in Zeolites J.L. Bonardet, M.C. Barrage and J.P. Fraissard	475
Investigations of Liquid-Phase Zeolite-Catalyzed Diels-Alder Reactions Ditha Hochgraeber-Paetow and Hans Lechert	483
Activity Enhancement of MeNaA Zeolites by Sulfiding with Hydrogen Sulfide for Acid-Catalyzed Reactions M. Sugioka, N. Sato and D. Uchida	493
Evolution of the Gallium Phase of Ga-H-MFI Aromatization Catalysts: Influence of Hydrogen J.F. Joly, H. Ajot, F. Alario, D. Ait Taleb, N.A. Gnep and M. Guisnet	501
Beckmann Rearrangement of Cyclohexanone Oxime over High Silica HZSM-5 Zeolites Modified with Boria T. Takahashi, T. Kai and M. Nishi	509
A Comparison of the Properties of MFI, Mordenite and Y Zeolites in Aromatic Transformations K. Ej-Jennane, Ch. Marcilly, C. Travers, J.F. Joly and E. Benazzi	517

Lateral-Chain Methylation of Toluene over Boron and/or Zinc Modified Cesium-X Zeolite D. Archier, G. Coudurier and C. Naccache	525
Catalytic Oxidative Dehydrogenation of Ethylbenzene to Styrene on Carbon Molecular Sieves P. Ciambelli, R.P. Dario and M. Turco	535
Acylation of Phenol and Transformation of Phenylacetate over Zeolites I. Neves, F.R. Ribeiro, J.P. Bodibo, Y. Pouilloux, M. Gubelmann, P. Magnoux, M. Guisnet and G. Perot	543
Catalytic Properties of [Al]-, [Ga]- and [Fe]-Silicate Analogs of ZSM-11 in C₇ and C₈ Aromatic Hydrocarbon Reactions: Influence of Isomorphous Substitution Anuj Raj, J. Sudhakar Reddy and Rajiv Kumar	551
Characterization of Dealuminated Mordenite by <i>n</i>-Decane Hydroconversion M.M. Olken and J.M. Garces	559
Comparison of Shape Selectivity of Coke Formation in Different Zeolites H. Schulz, W. Böhringer, and S. Zhao	567
Catalysis of Alkali Added Cu(II)-NaZ Zeolites in Benzyl Alcohol Oxidation H. Hayashibara, T. Nanbu, S. Nishiyama, S. Tsuruya and M. Masai	575
T.E.M. and Catalytic Property Study of Pt-Ga on HZSM-5 P. Mériaudeau, G. Sappaly and C. Naccache	583
Alkene Oligomerization Activity of Steam Dealuminated ZSM-5 B. Andersen, J.C.Q. Fletcher and C.T. O'Connor	591
Physico-Chemical Characterization and Catalytic Behavior of ZnO-NaZSM-5 Catalyst Bo-Qing Xu, Ming Yang, Juan Liang and Shi-Shan Sheng	599
Effect of the Crystallite Size of Titanium Silicalite-1 on the Activity in the Hydroxylation of Phenol A.J.H.P. van der Pol, A.J. Verduyn and J.H.C. van Hooff	607
Selective Hydrogenation with Pd(II)Salen Complexes Encaged in Y Type Zeolites D.E. de Vos and P.A. Jacobs	615

1-Pentene Isomerization over SAPO-11 and MeAPO-11 S.M. Yang and S.Y. Liu	623
The Synthesis of Pillared Nickel-Substituted Saponite and its Hydroisomerization Activity Dazhen Jiang, Tie Sun, Ziyang Liu, Enze Min and Mingyuan He	631
Beta Zeolite as Catalyst or Catalyst Additive for the Production of Olefins During Cracking of Gasoil L. Bonetto, A. Corma and E. Herrero	639
Basic Catalysis on Beta Zeotypes M.A. Cambor, A. Corma, R.M. Martin-Aranda and J. Perez-Pariente	647
DISCUSSION – Catalysis	655

Applications

Zeolites as Ceramics: Engineering New and Novel Ceramic Compositions and Microstructures From Molecular Sieves R.L. Bedard and E.M. Flanigen	667
Dynamics of Regenerative Zeolite Heat Exchangers Dimitar Tchernev	675
On the Innovation Potential of Aligned Molecular Sieve Crystals J. Caro, G. Finger, E. Jahn, J. Kornatowski, F. Marlow, M. Noack, L. Werner and B. Zibrowius	683
Preparation and Properties of a Metal Hydride/Zeolite Inclusion Jinping Li, Jinxiang Dong, Wenyang Xu and Feng Wu	693
Electrochemical and Electric-Field Effects at Dispersions of Zeolites Debra R. Rolison, Joseph Z. Stemple and David J. Curran	699
DISCUSSION – Applications	707
Author Index (Volumes I and II)	709
Subject Index (Volumes I and II)	715

SYNTHESIS OF OLIGO- AND POLYTHIOPHENES IN ZEOLITE HOSTS

Patricia ENZEL[#] and Thomas BEIN

Department of Chemistry, Purdue University, West Lafayette, IN 47907, USA

[#] Present Address: Lash Miller Chemical Laboratories, University of Toronto, 80 St. George Street, Toronto, Ontario, M5S 1A1, Canada

ABSTRACT

Oligomers and polymers of thiophene derivatives were synthesized in the channels of zeolite Y and mordenite. Intrazeolite oxidation of monomers such as thiophene, 3-methylthiophene, and bithiophene by Fe(III) or Cu(II) ions results in formation of insoluble polymers that have spectroscopic properties similar to the corresponding bulk polymers. The zeolites containing the polymers are nonconducting, but when extracted from the host, the polymers show d.c. conductivities typical for the bulk materials. Oligothiophene species with well-defined electronic transitions could be produced in acidic zeolite Y.

INTRODUCTION

The synthesis of molecule-based conducting materials has attracted growing interest due to their potential for applications in microelectronics and electrical components such as batteries.¹ Work in this laboratory has recently demonstrated the encapsulation of conjugated polymers such as polypyrrole, polyaniline and polythiophene in the crystalline channel systems of large-pore zeolites.² Precursor monomers are introduced into the zeolite host and are subsequently polymerized by appropriate oxidants in the pore system.

Other inclusion techniques, e.g., growth of polymer fibers in membranes,³ and intercalation of pyrrole in layered vanadium oxide⁴ have recently been explored. Methylacetylene gas was found to react with the acid sites in zeolites L, Y, beta, ZSM-5, omega, mordenite, and SAPO-5 to form reactive, conjugated oligomers⁵. Short-chain oligomers of polythiophene were prepared in Na-pentasil zeolites⁶. In the latter study it was found that the presence of aluminum in the zeolite framework is essential for oxidation, but the cause for the formation of the cationic species remained unresolved.

The present article addresses the polymerization of different thiophenes and the question of the active site in the formation of oligothiophene species in large-pore zeolites. Spectroscopic measurements show that the presence of Bronsted sites is essential for the formation of the same oligothiophene species as observed by Caspar et al. in ZSM-5.⁶

In the chemical synthesis of polythiophene (PTh)^{7,8}, the direct oxidation of the monomers with Fe(ClO₄)₃ or Cu(ClO₄)₂, produces the corresponding doped polymers. The polymerization reaction involves removal of 2.25 to 2.50 electrons per molecule of thiophene. The resulting polymer is produced in the oxidized state with 0.25 to 0.50 positive charges per thiophene unit, depending on the synthesis conditions.

EXPERIMENTAL

NaY (LZY-52), NH₄Y (LZY-62), and Na-mordenite (LZ-M5) were generously donated by the Union Carbide Corporation. Zeolite A (5A) was obtained from Alfa. The zeolites were dehydrated in a flow of oxygen (1 °C/min to 100 °C, 10 h at 100 °C, and 8 h at 400 °C (4 h under vacuum)). Fe^{III} and Cu^{II} zeolites were prepared according to conventional ion-exchange and oxidation techniques⁹. The resulting zeolite unit cell compositions are: Cu^{II}Y: Cu₁₅Na₂₆(AlO₂)₅₆(SiO₂)₁₃₆, Fe^{III}Y: Fe₁₂Na₃₂(AlO₂)₅₆(SiO₂)₁₃₆, Cu^{II}M: Cu_{2.5}Na₃(AlO₂)₈(SiO₂)₄₀, Cu^{II}A: Cu₈Na₈₀(AlO₂)₉₆(SiO₂)₁₉₂.

2,2'-Bithiophene (BTh) and terthiophene (TTh) were introduced into the zeolites from a hexane solution. The zeolites used were NaY, H₂Y, H₆Y (2 and 6 protons per supercage/ β -cage), and Fe^{III}Y. Typically, 0.5 g of zeolite was mixed with 20 ml of hexane containing 0.01 g of the oligomer (0.06 mmol 2,2'-bithiophene, or 0.04 mmol terthiophene), stirred for 12 hours, washed with an excess of hexane, and dried under nitrogen. The other monomers were introduced into the zeolites from solutions in water, chloroform, acetonitrile, hexane, toluene, or from the vapor-phase. Bulk-like polymers could be recovered from the zeolites after dissolution of the framework with a 25% aqueous solution of HF. Polythiophene and poly(3-methylthiophene) are not attacked in acidic media¹⁴. Additionally, a blank experiment shows that the monomers do not polymerize after exposure to acids for 24 hours. Bulk polymers were prepared chemically by oxidative polymerization with Fe(ClO₄)₃ in MeCN.

RESULTS AND DISCUSSION

Intrazeolite polymerization. If thiophene monomers are admitted into the Fe^{III} or Cu^{II} forms of zeolites Y or mordenite from the vapor phase or from hexane and toluene solutions (Table 1), the colors of the resultant adducts change slowly (within 30-120 min) from white to different shades of blue or dark green. These color changes correspond to those observed in bulk polymerization. Thiophene monomers in zeolite containing only sodium ions do not react to form polymers, due to the absence of oxidation centers.

No polymer formation is observed with Cu^{II}A, with a pore size of 4.1 Å, which is too small for the thiophene monomers. The monomers have a kinetic diameter of approximately 6 Å and can not diffuse into the zeolite cavities, where the majority of the oxidant ions are located. In contrast to trends observed in the bulk polymerization reactions, polar solvents such as water, acetonitrile, and chloroform do not favor the intrazeolite polymerization of thiophene and 3-methylthiophene. The intrazeolite metal ions are probably screened by the polar solvent molecules. From the estimated surface capacity of the zeolite crystals, 0.2 molecules per unit cell of zeolite Y (based on 1 μ m crystals), and the observed monomer loadings (Table 1), it can be concluded that most of the monomer molecules are introduced into the pore system of the zeolite

host. Scanning electron micrographs indicate no evidence of polymer covering the surfaces of zeolite/polymer crystals. Pyrolysis mass spectrometry detects considerably less monomer evolution from the zeolite/polymer samples than from those containing unreacted monomers in the Na-forms, as expected if polymerization has taken place. The above observations demonstrate that the polythiophene chains form within the zeolite pore systems.

After dissolution of the framework ($\text{Cu}^{\text{II}}\text{Y-3MTh-V}$) with an aqueous solution of HF, a black powder is obtained with a 16 % yield, based on the amount of monomer loaded into the zeolite. In the case of $\text{Cu}^{\text{II}}\text{Y-3MTh-V}$, this value corresponds to 5 molecules of 3-methylthiophene reacted per unit cell of zeolite, which corresponds well to the 2.3 to 1 ratio of oxidant to monomer necessary for oxidative polymerization.

Table 1: Zeolite/thiophene and 3-methylthiophene samples

Sample	Monomer loaded per unit cell		Product color
	Th ^a	3MTh ^a	
NaY--V	37	30.5	white
NaY--H	5.6 (6.5)*	5.6 (6.5)*	white
$\text{Cu}^{\text{II}}\text{Y--V}$	35	32	dark blue
$\text{Cu}^{\text{II}}\text{Y--W}$	5.6 (6.5)*	5.6 (6.5)*	white
$\text{Cu}^{\text{II}}\text{Y--H}$	5.4 (6.5)*	5.7 (6.5)*	dark blue
$\text{Fe}^{\text{III}}\text{Y--V}$	29	25	dark green
NaM--V	2	2	white
NaM--H	1 (1)*	1 (1)*	white
$\text{Cu}^{\text{II}}\text{M--V}$	1.5	1	blue-grey
$\text{Cu}^{\text{II}}\text{M--W}$	1 (1)*	1 (1)*	white
$\text{Cu}^{\text{II}}\text{M--H}$	1 (1)*	1 (1)*	blue
$\text{Fe}^{\text{II}}\text{M--V}$	1	1	grey-green
$\text{Cu}^{\text{II}}\text{A--V}$		0.2	light blue

^a Abbreviations: Y, zeolite Y; M, mordenite; Th, thiophene; 3MTh, 3-methylthiophene; V, vapor; H, hexane (similar with toluene); and W, water (similar with acetonitrile, chloroform).
* The numbers in parentheses correspond to the amount of monomers dosed from solution to achieve 2.3:1 oxidant to monomer stoichiometry.

Spectroscopic characterization. The IR spectra of $\text{Fe}^{\text{III}}\text{Y-3MTh-V}$ and of $\text{Cu}^{\text{II}}\text{Y-3MTh-V}^{2b}$ show typical vibrations of poly(3-methylthiophene)^{10,11}. The weak band at 1506 cm^{-1} is assigned to aromatic C=C stretching vibrations, and two strong bands around 1400 , and 1331 cm^{-1} are related to the heterocycle C-N stretching vibrations (Figure 1). The presence of the intense, fairly broad bands at 1400 and 1331 cm^{-1} indicates that the polymer chains are in the oxidized form. At higher energy (not shown), the spectra also exhibit a characteristic tail of the electronic transition correlated with the presence of free carriers in highly conducting polythiophenes¹². The IR spectra of the black agglomerated products extracted from the zeolites and those of the

zeolite/polythiophene samples are comparable to the IR spectra of chemically synthesized bulk materials.

Neutral poly(3-methylthiophene) (and polythiophene) films formed electrochemically show absorption in the visible region at about 2.5 eV, associated with the $\pi \rightarrow \pi^*$ transition of long conjugated polymer chains^{13,14}. When the bulk polymer is oxidized, two intra-gap absorptions associated with bipolarons develop at about 0.65 and 1.6 eV. With progressive oxidation, the 2.5 eV absorption decreases in intensity. A representative zeolite sample, Cu^{II}Y-Th-V, shows corresponding features at about 440 nm (ca. 2.8 eV), 670 nm (1.9 eV), and a broad absorption between ca. 1.4 and 0.25 eV (see also Figure 2C). Similar features are observed with the Fe^{III}-containing hosts and with 3MPTh-loaded zeolites. If the NIR absorption of these samples is compared with data for thiophene nonamers (9^{2+})⁶, it can be concluded that the intrazeolite polymer chains should be much longer than 10 units.

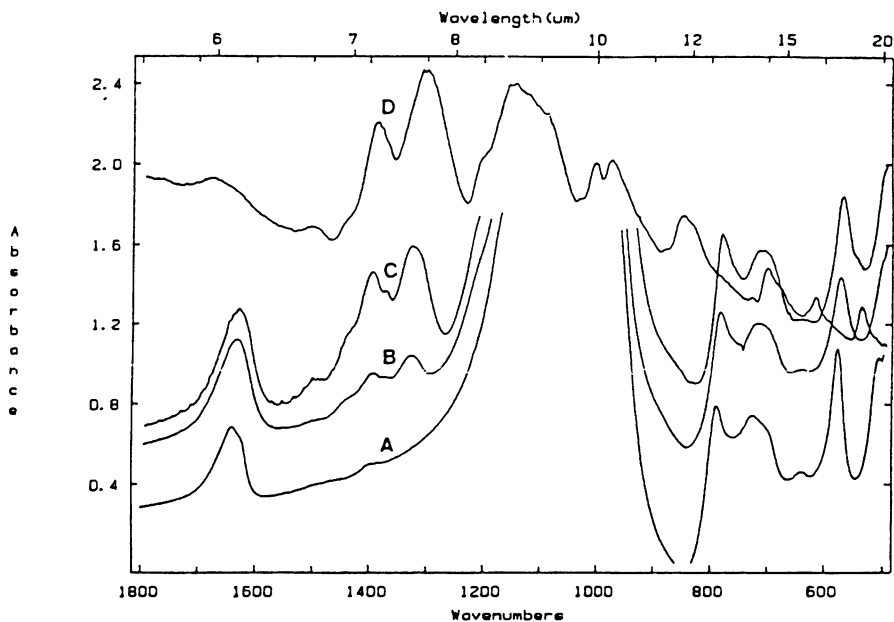


Figure 1. FTIR spectra of poly(3-methylthiophene) samples. (A) NaY, (B) Fe^{III}Y-3MTh-V, (C) Cu^{II}Y-3MTh-V, and (D) bulk poly(3-methylthiophene).

The ESR spectra of the Cu^{II}-PTh samples present signals at $g=2.0027$. This value is typical of a delocalized carbon-based radical¹⁵. The signals are rather broad, with bandwidths greater than 6 Gauss, characteristic of localized radical spins and an indication of interaction of the encapsulated polymer with the zeolite hosts. The presence of only about 2.0×10^{-3} spins per monomer is consistent with the existence of bipolarons as charge carriers. Pressed zeolite/polymer pellets show no significant 'bulk' conductivity, with $\sigma < 10^{-8} \text{ Scm}^{-1}$. Therefore, there is no significant deposition of polymer on the external crystal surfaces. Agglomerated P3MTh recovered from Cu^{II}Y-3MTh-V after dissolution of the host shows a conductivity of about 0.01 Scm^{-1} . This value is close to that obtained for poly(3-methylthiophene) synthesized by chemical methods.

Stabilization of thiophene oligomers within zeolites. In a recent study, thiophene oligomers were formed within the channels of zeolite beta and Na-ZSM-5⁶. Charged short-chain oligomers are inherently reactive species, and in the particular case of polythiophene, oxidized oligomers are unstable with respect to further oligomerization in solution. Thus, the zeolite is an excellent matrix to stabilize them. One of the questions that the above study did not address relates to the nature of the reactive sites and the reaction mechanism in the zeolite, since the oligomers were formed without any traditional oxidant, such as ferric or cupric ions.

A related polyheterocycle, polypyrrole, is known to form in the presence of protonic acids¹⁶. Accordingly, one might assume that the formation of polythiophene could proceed through the same mechanism as in polypyrrole. We propose that the presence of acid groups in the zeolite is responsible for the formation of the thiophene oligomers. To test this assumption, short oligomers of thiophene (Th), bithiophene (BTh) and terthiophene (TTh), were loaded from hexane into the acid and Fe^{III} forms of zeolite Y. Different concentrations of protons per unit cell of zeolite Y, H₁₆Na₄₀Y (H₂Y) and H₄₈Na₈Y (H₆Y) were used to study the effect of proton stoichiometry on the products formed. After a few minutes a change in color was noticeable in the zeolites, but to drive the reaction to completion, it was continued for 12 hours. NaY-monomer adducts produced only minor but detectable spectral changes.

H₂Y and H₆Y zeolites loaded with bithiophene yield a yellow-green complex. The same zeolites loaded with terthiophene produce an intense purple complex. These colors are very different from the green-black color obtained when thiophene, bithiophene, or terthiophene were loaded in Fe^{III}Y, where polymerization to polythiophene takes place. The main features of the UV/VIS/NIR reflectance spectra (Figure 2) and their assignments to different oligomer cations according to ref. [6] are summarized in Table 3. It is not quite clear if the species observed here are radical cations, dications, or rather protonated heterocycles. Related studies¹⁷ on these and other monomers suggest the formation of protonated species.

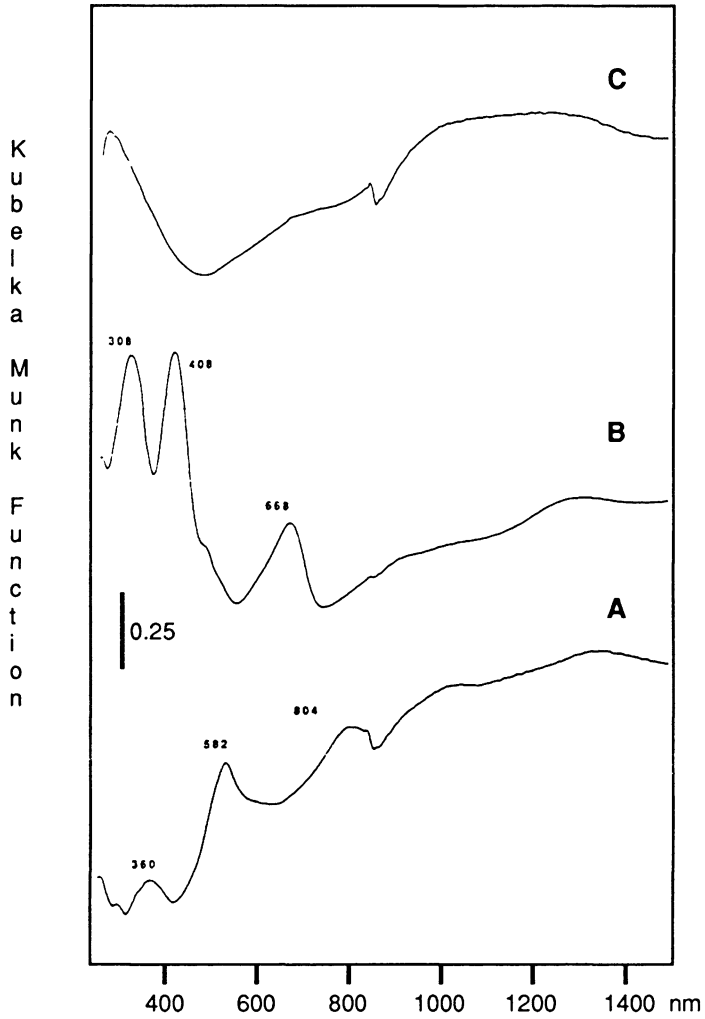


Figure 2. UV/VIS/NIR reflectance spectra of thiophene oligomers in acid zeolites. (A) H6Y-TTh-H, (B) H6Y-BTh-H, and (C) Fe(III)Y-BTh-H. The feature at 850 nm is an artifact due to change of detectors.

Table 3: UV/VIS/NIR bands for thiophene oligomers in zeolite Y^a

Sample	Band Positions (nm) and Assignments (after reference 6, in parentheses)			
Fe ^{III} Y-Th-H		470sh	$\pi-\pi^*$ in neutral PTh	broad NIR band oxidized PTh
NaY-BTh-H	308s	402sh	678w	
	2(300)	2 ^{o+} (407)	8 ²⁺ (661)	
H ₂ Y-BTh-H	308s	408s	668s	1274 broad
	2	2 ^{o+}	8 ²⁺	8 ²⁺ ... (1383)
H ₆ Y-BTh-H	308s	408s	668s	1300 broad
	2	2 ^{o+}	8 ²⁺	8 ²⁺ ...
Fe ^{III} Y-BTh-H				broad NIR band oxidized PTh
NaY-TTh-H	370s	528sh		
	3(354)	3 ^{o+} (522)		
H ₂ Y-TTh-H	360s	532s	788s	broad NIR band
	3	3 ^{o+}	6 ^{o+} (775)	oxidized PTh
H ₆ Y-TTh-H	360s	528s	804s	1024 + broad NIR
	3	3 ^{o+}	6 ^{o+} or 3 ²⁺ (833)	6 ²⁺ +ox. PTh
Fe ^{III} Y-TTh-H				broad NIR band oxidized PTh

^a 2, neutral bithiophene; 2⁺, bithiophene radical cation; 3, neutral terthiophene; 3⁺, terthiophene radical cation; 6⁺, hexathiophene radical cation; 6²⁺, hexathiophene dication; 8²⁺, octathiophene dication. H, hexane; sh, shoulder; s, strong; and w, weak.

The strong bands at about 308 nm for the bithiophene loaded zeolites and at 360 nm for the terthiophene loaded zeolites correspond to the band gap transition in the neutral oligomer⁶. In the spectra of NaY zeolites loaded with these monomers, the above bands are dominant. Distinctive bands at lower energies, only present in the acid zeolites, are tentatively assigned to radical cations and dications typical of the thiophene oligomers. Bithiophene can form a stable radical cation, 2⁺, in acid zeolites as shown by the band at 408 nm. Additionally, two bands at 668 nm and at about 1300 nm, assigned to the octamer dication 8²⁺, are present in the spectra (Figure 2, B). For terthiophene, a band at 528 nm assigned to the radical cation 3⁺, and a band around 800 nm related to the hexamer 6⁺ are observed (Figure 2, A). The spectra of Fe^{III}Y-BTh and Fe^{III}Y-TTh are very similar to the spectrum of Fe^{III}Y-Th, in which the main spectral characteristic is a broad absorption band extending into the near-IR, assigned to the oxidized form of polythiophene (Figure 2, C). It is important to note that the spectra of the adducts in acid zeolite show also the broad near IR absorption typical for the polymer, which indicates the concomitant formation of oligomers and polymers in the zeolites.

The distinctive bands related to radical cations and dications of short oligomers of thiophene in zeolites are only observed in the presence of protons. These results can also explain the formation of the same species in Na-ZSM-5 since this zeolite can contain a small

amount of protons as well. However, the reactivity of the thiophene species in proton vs. Fe^{III} zeolite forms is still not completely understood. If a strong oxidant ion is present in the zeolite, such as Fe^{III}, the oxidation is driven to completion forming oxidized polymers. The reaction pathway is apparently a function of the oxidation potential of the oxidant.

CONCLUSIONS

In summary, this study demonstrates that it is possible to polymerize thiophene, 3-methylthiophene, and small oligomers within the channel systems of zeolites, analogous to the oxidative coupling of thiophene and 3-methylthiophene in solution in the presence of Cu^{II} and Fe^{III} oxidants. Oligomerization and polymerization reactions proceed to different degrees in acidic and oxidant-containing zeolites.

ACKNOWLEDGEMENTS

The authors thank Dr. Francois Beuneu (Ecole Polytechnique, Paris) for taking the ESR spectra. Partial funding for this work from Sprague Electric Company is appreciated.

REFERENCES

- 1 Proceedings of the International Conference on Science and Technology of Synthetic Metals, ICSM '88 and '90; *Synth. Metals*, **28** (1-3) and **29**(1) (1988), and *Synth. Metals*, **41-43** (1991).
- 2 (a) P. Enzel, T. Bein, *J. Phys. Chem.*, **93**, 6270 (1989). (b) P. Enzel, T. Bein, *J. Chem. Soc., Chem. Commun.*, 1326 (1989). (c) T. Bein, P. Enzel, *Angew. Chem., Int. Ed. Engl.*, **28**, 1692 (1989). (e) T. Bein, P. Enzel, F. Beuneu, L. Zuppiroli, *ACS Adv. Chem. Ser.*, No. **226**, p. 433 (1990).
- 3 Z. Cai, and C. R. Martin, *J. Am. Chem. Soc.*, **111**, 4138 (1989).
- 4 M. G. Kanatzidis, C.-G. Wu, H. O. Marcy, and C. R. Kannewurf, *J. Am. Chem. Soc.*, **111**, 4139 (1989).
- 5 S. D. Cox, and G. D. Stucky, *J. Phys. Chem.*, **95**, 710 (1991).
- 6 J. V. Caspar, V. Ramamurthy, and D. R. Corbin, *J. Am. Chem. Soc.*, **113**, 600 (1991).
- 7 N. Mermilliod-Thevenin, and G. Bidan, *Mol. Cryst. Liq. Cryst.*, **118**, 227 (1985).
- 8 M. B. Inoue, E. F. Velazquez, and M. Inoue, *Synth. Metals*, **24**, 223 (1988).
- 9 J. R. Pearce, W. J. Mortier, J. B. Uytterhoeven, and J. H. Lunford, *J. Chem. Soc., Faraday Trans. 1*, **77**, 937 (1981).
- 10 H. Neugebauer, G. Nauer, A. Neckel, G. Tourillon, F. Garnier, and P. Lang, *J. Phys. Chem.*, **88**, 652 (1984).
- 11 J. E. Osterholm, P. Sunila, and T. Hjerberg, *Synth. Metals*, **18**, 169 (1987).
- 12 S. Hotta, W. Shimotsuma, and M. Taketani, *Synth. Metals*, **10**, 85 (1984/5).
- 13 G. Dian, G. Barbey, and B. Decroix, *Synth. Metals*, **24**, 223 (1988).
- 14 N. Colaneri, M. Nowak, D. Spiegel, S. Hotta, A. J. Heeger, *Phys. Rev. B*, **36**, 7964 (1987).
- 15 D. P. Murray, L. D. Kispert, and S. Petrovic, *Synth. Metals*, **28**, C269 (1989).
- 16 M. Salmon, K. K. Kanazawa, A. F. Diaz, and M. Krounbi, *J. Polym. Sci., Polym. Lett. Ed.*, **20**, 187 (1982).
- 17 R. J. Gorte, personal communication.